Electrocatalytic sensor devices: (I) cyclopentadienylnickel(II) thiolato Schiff base monolayer self-assembled on gold[☆]

Aoife Morrin [a,b], Richard M. Moutloali [a], Anthony J. Killard [b], Malcolm R. Smyth [b], James Darkwa [a], Emmanuel I. Iwuoha [a,*]

[a] *Department of Chemistry, University of the Western Cape, Bellville 7535, South Africa*
[b] *School of Chemical Sciences, Dublin City University, Dublin 9, Ireland*

Abstract

The fabrication of a self-assembled monolayer (SAM) of a cyclopentadienylnickel(II) thiolato Schiff base compound, $[\text{Ni}(\text{SC}_6\text{H}_4\text{NC}(\text{H})\text{C}_6\text{H}_4\text{OCH}_2\text{CH}_2\text{SMe})(\eta^5\text{-C}_5\text{H}_5)]_2$ on a gold electrode is described. Effective electronic communication between the Ni(II) centres and the gold surface was established by electrochemically cycling the Schiff base-doped Au electrode in 0.1 M NaOH from $-200\,\text{mV}$ to $+600\,\text{mV}$. The SAM-modified electrode exhibited quasi-reversible electrochemistry. The integrity of this electrocatalytic SAM, with respect to its ability to block and electro-catalyse certain Faradaic processes, was interrogated using cyclic voltammetric experiments. The formal potential, $E^{\circ\prime}$, varied with pH to give a slope of about $-30\,\text{mV}\,\text{pH}^{-1}$. The surface concentration, G, of the nickel redox centres was found to be $1.548 \times 10^{-11}\,\text{mol}\,\text{cm}^{-2}$. By electrostatically doping the SAM using an applied potential of $+700\,\text{mV}$ versus Ag/AgCl, in the presence of horseradish peroxidase (HRP), it was fine-tuned for amperometric determination of H_2O_2. The electrocatalytic-type biosensor displayed typical Michaelis–Menten kinetics and the limit of detection was found to be 6.25 mM.

1. Introduction

Different strategies have been employed for the formation of monolayers on electrode surfaces, such as Langmuir–Blodgett (LB) transfer [1] and self-assembly techniques [2]. Although LB films formed by physisorption of amphiphiles have been applied successfully to biosensors, they are thermodynamically unstable, and consequently minor changes in temperature, or exposure to solvent can ruin their two dimensional structure [3]. SAM formation, pioneered by Nuzzo and Allara in 1983 [4], on the other hand, give more rugged films, due to the strong chemisorption of suitable molecules like organo-sulphur compounds onto noble metals. The formation of SAMs on gold electrodes have yielded very promising results for the construction of electrochemical biosensors, the advantages of which are: (i) improved electrocatalysis, (ii) freedom from surface fouling and (iii) prevention of undesirable reactions competing kinetically with the desired electrode process [5]. Particular emphasis has been placed on alkanethiol monolayers [6–8], which are known to form well-ordered assemblies that can be used to immobilise protein close to the electrode surface with a high degree of control over the molecular architecture of the recognition interface. Alkanethiols have also been modified to include electroactive moieties (for mediator or electron transfer function), so that the SAMs can be used for electrical wiring or communication between the redox active enzymes and the electrode surface. Several of these alkanethiols functionalised with electron transfer mediators such as tetrathiafulvalene [9] and viologen [10] have been applied to biosensing.

In this study a novel cyclopentadienylnickel(II) compound $[\text{Ni}(\text{SC}_6\text{H}_4\text{NC}(\text{H})\text{C}_6\text{H}_4\text{OCH}_2\text{CH}_2\text{SMe})(\eta^5\text{-C}_5\text{H}_5)]_2$ has been used as the active redox centre for our SAM layer. This was in part due to the reversible redox behaviour found

for such compounds. For example, Ho and Mak [11] have found that compounds of the type [Ni(Cp)$_2$(SR)$_2$], where R = Ph or PhCH, have reversible redox couples at low positive potentials. Recently, we have extended the study to Schiff base analogues of the compounds mentioned in the work of Ho and Mak, and have obtained similar results [12]. These complexes exhibit low positive formal potentials ($E^{\circ\prime}$) versus normal hydrogen electrode (NHE) and are inert to moisture and air, thus, making them suitable candidates for SAM applications in sensors, in particular, biosensors. Electrocatalytically active electrode surfaces of this type provide reagentless platforms for enzyme catalysis. Various electrode configurations for electrocatalytically configuring the electrode surface based on immobilised molecular redox couples [10,13,14], or redox polymers [15–17] have been described. When compared to systems based on direct electron transfer (DET) between the active site of the enzyme and the electrode, that is, in the absence of electrode bound redox moieties, electrocatalytically active surfaces have the advantages of being more versatile and possess greater efficiency in terms of electron transfer rates [18].

In this work, fundamental characterisation of a cyclopentadienylnickel(II) thiolato Schiff base compound, [Ni(SC$_6$H$_4$NC(H)C$_6$H$_4$OCH$_2$CH$_2$SMe)(η^5-C$_5$H$_5$)]$_2$, was probed, and its SAM analogue interrogated, using electrochemical techniques. To assess this SAM's efficiency in an electrocatalytic biosensor device, horseradish peroxidase (HRP) was chosen as a model enzyme for catalysis of hydrogen peroxide. HRP was electrostatically applied to the surface of the SAM and electrochemical reduction of H$_2$O$_2$ present in solution was carried out. The sensor was characterised in terms of detection limit, K_m^{app} and I_{max}.

2. Experimental

2.1. Materials

Tetrabutylammonium tetrafluoroborate (TBATFB, 21,796-4); horseradish peroxidase (1.110 U mg^{-1}, P6782) and 30% (v/v) hydrogen peroxide solution (31642) were purchased from Sigma-Aldrich. Dichloromethane and acetone were purchased from B and M Scientific (South Africa). All other reagents were of analytical grade and were used as obtained from the suppliers without further purification.

2.2. Buffers and solutions

All electrochemical measurements were carried out in phosphate buffered saline (PBS), (0.1 M phosphate, 0.137 M NaCl and 2.7 mM KCl), pH 7.4, unless otherwise stated.

2.3. Synthesis

2.3.1. Synthesis of OHCC$_6$H$_4$OCH$_2$CH$_2$SMe (1)
4-Hydroxybenzaldehyde (1.0 g, 8.19 mmol) was dissolved in acetone and then charged with finely ground K$_2$CO$_3$ (5 g). 1-Chloroethylmethylsulphide (1.82 ml, 16.38 mmol) was added to the mixture. The reaction mixture was refluxed for 48 h. The mixture was filtered and the solvent removed from filtrate to leave a pale orange–yellow liquid. Yield = 1.56 g, 97%. ^{1}H NMR (CDCl$_3$): δ 9.89 (s, 1H, CHO), 7.84 (d, 2H, J_{HH} = 8.2 Hz, OHCC$_6$H$_4$), 7.00 (d, 2H, J_{HH} = 8.6 Hz, OC$_6$H$_4$), 4.24 (t, 2H, OCH$_2$), 2.88 (t, 2H, SCH$_2$), 2.22 (s, 3H, SCH$_3$).

2.3.2. Synthesis of HSC$_6$H$_4$NC(H)C$_6$H$_4$OCH$_2$ CH$_2$SMe (2)
4-Aminothiophenol (0.34 g, 2.71 mmol) and compound 1 (0.5 ml, 2.71 mmol) were dissolved in toluene (50 ml). Acetic acid (two drops) was added to the solution and the reaction left for 18 h at room temperature. Solvent was removed from the solution to leave a yellow residue which was crystallised from CH$_2$Cl$_2$:hexane (1:3) mixture at -15 °C. A yellow precipitate was isolated. Yield = 0.41 g, 50%. ^{1}H NMR (CDCl$_3$): δ 8.36 (s, 1H, C(H)N), 7.81 (d, 2H, J_{HH} = 8.4 Hz, C(H)C$_6$H$_4$), 7.30 (d, 2H, J_{HH} = 8.2 Hz, NC$_6$H$_4$), 7.14 (d, 2H, J_{HH} = 8.4 Hz, OC$_6$H$_4$), 7.00 (d, 2H, J_{HH} = 8.4 Hz, SC$_6$H$_4$), 4.22 (t, 2H, OCH$_2$), 2.91 (t, 2H, SCH$_2$), 2.23 (s, 3H, SCH$_3$).

2.3.3. Synthesis of [Ni(SC$_6$H$_4$NC(H)C$_6$H$_4$OCH$_2$CH$_2$SMe) (η^5-C$_5$H$_5$)]$_2$ (3)
A mixture of compound 2 (0.3 g, 0.99 mmol) and nickelocene (0.19 g, 0.99 mmol) were dissolved in toluene (40 ml) to give a green solution. The reaction was left for 18 h and the colour gradually turned brown–black. The mixture was filtered and the filtrate concentrated to half the original volume and hexane (40 ml) added. The solution was stored at -15 °C to form a black precipitate. Yield = 0.11 g, 24% ^{1}H NMR (CDCl$_3$): δ 0.8.44 (s, 2H, C(H)N), 8.10 (d, 4H, J_{HH} = 8.6 Hz, C(H)C$_6$H$_4$), 7.88 (d, 4H, J_{HH} = 8.6 Hz, NC$_6$H$_4$), 7.04 (dd, 8H, SC$_6$H$_4$, OC$_6$H$_4$), 4.63 (s, 10H, C$_5$H$_5$), 4.24 (t, 4H, OCH$_2$), 2.94 (t, 4H, SCH$_2$), 2.25 (s, 6H, SCH$_3$). Anal. calcd. for C$_{42}$H$_{56}$N$_2$O$_2$S$_4$Ni$_2$: C, 58.22; H, 6.51; N, 3.23%. Found C, 58.61; H, 4.55; N, 3.59%.

2.4. Instrumentation

All electrochemical protocols were performed on a BAS50/W electrochemical analyser with BAS 50/W software, using either cyclic voltammetry (CV), Oysteryoung square wave voltammetry (OSWV) or time-based amperometric modes. A conventional three electrode system was employed. The working electrodes (WE) were gold disc electrodes from Cypress Systems (diameter: 1.0 mm), and Bioanalytical Systems (diameter: 1.5 mm). Silver/silver chloride (Ag/AgCl) and a platinum wire were used as reference and auxiliary electrodes, respectively. For convention, a negative oxidation current was used for the display of all figures.

All cyclic voltammograms were carried out at a scan rate of 50 mV s^{-1}, unless otherwise stated. Square wave voltam-

mograms were carried out using a step potential of 4 mV, an amplitude of 25 mV, and a frequency of 15 Hz.

2.5. Preparation of cyclopentadienylnickel(II) thiolato Schiff base monolayer on gold electrode

Prior to use, gold electrodes were first polished on aqueous slurries of 1, 0.3 and 0.05 μm alumina powder. After thorough rinsing in deionised water followed by acetone, the electrodes were etched for about 5 min in a hot 'Piranha' solution {1:3 (v/v) 30% H_2O_2 and concentrated H_2SO_4} and rinsed again with copious amounts of deionised water and then deposition solvent, CH_2Cl_2. Finally the electrode was placed in a solution of 0.5 M H_2SO_4 and 10 voltammetric cycles were carried out between −1200 and 1500 mV at 50 mV s^{-1} versus Ag/AgCl. Following this pre-treatment, the electrode was rinsed with CH_2Cl_2, and immediately placed in a 1 ml solution of [Ni(SC$_6$H$_4$NC(H)C$_6$H$_4$OCH$_2$CH$_2$SMe)(η^5-C$_5$H$_5$)]$_2$ (1×10^{-3} mol dm^{-3}) for 24 h at room temperature. Upon removal from the CH_2Cl_2 deposition solution, the electrode was thoroughly rinsed with CH_2Cl_2. Finally, in order to observe redox activity of the SAM, a voltammetric cycle in 0.1 M NaOH between −200 and +600 mV versus Ag/AgCl was required.

2.6. Immobilisation of protein

Following SAM preparation, the electrode was transferred to a 1 ml batch cell. The surface of the SAM was oxidised in 0.1 M phosphate buffer solution, pH 7.4, in the presence of HRP (1 mg ml^{-1}) at +700 mV versus Ag/AgCl, sample interval of 500 ms, over 1500 s at a sensitivity of 1×10^{-9} A V^{-1}. During this oxidation, the enzyme becomes electrostatically attached to the SAM surface. The enzyme solution was carefully recovered from the cell, and re-stored for later use.

3. Results and discussion

3.1. Electrochemical characterisation of the cyclopentadienylnickel(II) thiolato Schiff base compound in solution

It had previously been observed, that cyclopentadienylnickel(II) thiolato Schiff base compounds of the form [Ni(SC$_6$H$_4$NC(H)C$_6$H$_4$OC$_n$H$_{2n+1}$)(η^5-C$_5$H$_5$)]$_2$, where $n = 4$, 14 and 16, exhibit ideal reversible electrochemistry, with low positive $E^{\circ\prime}$ values versus NHE [12], making them ideal candidates for electron transfer mediators in biosensors. Hence, a thiol-derivatised cyclopentadienylnickel(II) thiolato Shiff base, [Ni(SC$_6$H$_4$NC(H)C$_6$H$_4$OCH$_2$CH$_2$SMe)(η^5-C$_5$H$_5$)]$_2$, was synthesised, (Section 2.3), for the fabrication of a redox active self-assembled monolayer (SAM) on a gold electrode. The redox properties of this new com-
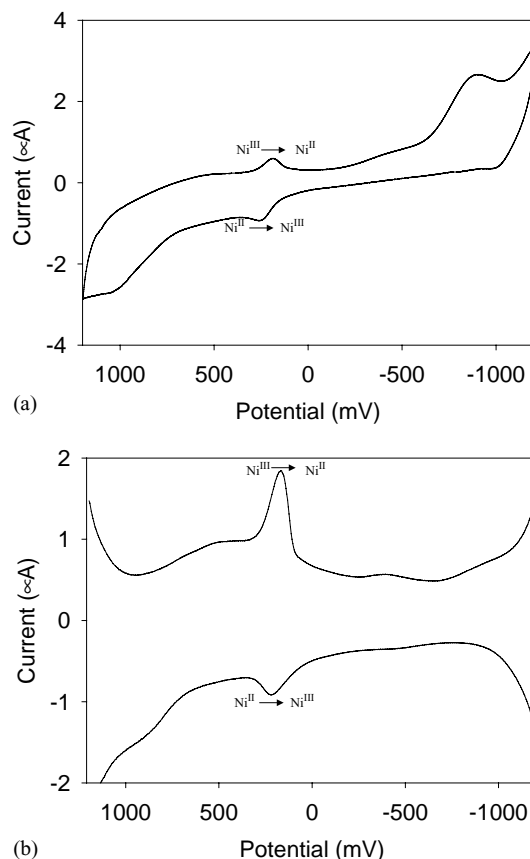

Fig. 1. (a) Cyclic (50 mV s^{-1} scan rate) and (b) square wave (4 mV step potential, 25 mV amplitude, 15 Hz frequency) voltammograms for 2×10^{-3} M [Ni(SC$_6$H$_4$NC(H)C$_6$H$_4$OCH$_2$CH$_2$SMe)(η^5-C$_5$H$_5$)]$_2$ on a 1.0 mm diameter bare gold disk electrode in CH_2Cl_2 containing 0.1 M TBATFB.

plex were studied under stationary conditions at a gold disk electrode using cyclic voltammetry and Oysteryoung square wave voltammetry in CH_2Cl_2 containing TBATFB (0.1 M). The concentration employed for the experiments was 2×10^{-3} mol dm^{-3}. The CV shows a prominent redox wave with a formal potential, $E^{\circ\prime}$, of +203 mV versus Ag/AgCl using a scan rate of 50 mV s^{-1}, which was attributed to the Ni^{II}/Ni^{III} redox couple (Fig. 1a). The oxidation peak at −800 mV could be attributed to production of Ni^{IV}, or may be ligand-based. Fig. 1b displays the OSWV of the complex, which also shows the electrochemistry of the Ni^{II}/Ni^{III} redox couple. Sweeping the electrode through potentials outside of its potential window can deteriorate the behaviour of the system, due to formation of oxides or hydrogen evolution at the working electrode. Therefore, although the Ni^{II}/Ni^{III} redox peaks appeared only to be quasi-reversible under these conditions, it was shown to be reversible when the potential was swept over a narrower range to isolate this redox couple (see below). The purpose of sweeping the potential over a wide range was to survey all the electrochemistry of the complex. It was seen that the Ni^{II}/Ni^{III} redox electrochemistry was the only activity present in the complex warranting further characterisation.

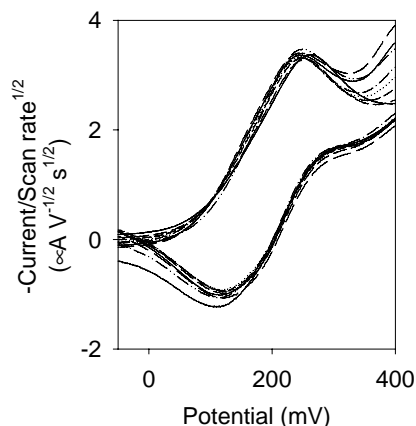Fig. 2. Reversibility plots for the voltammograms of 2×10^{-3} M [Ni(SC$_6$H$_4$NC(H)C$_6$H$_4$OCH$_2$CH$_2$SMe)(η^5-C$_5$H$_5$)]$_2$ from -200 to $+600$ mV. The scan rate was varied from 20 to 250 mV s^{-1}. Other conditions are as in Fig. 1. (All plots superimposed, demonstrating the reversibility of the Ni^{II}/Ni^{III} redox couple).

Fig. 2 is a plot of $-I\upsilon^{-1/2}$ versus E for voltammograms of the Ni^{II}/Ni^{III} redox couple for varying scan rates. Plots of this nature should superimpose at all scan rates for a reversible couple [19], that is, if peak current is proportional to $\upsilon^{-1/2}$, and ΔE_p remains constant with varying υ. In this case, the potential was swept from -200 to $+600$ mV at scan rates ranging from 20 to 250 mV s^{-1}. All plots were normalised to correct for double-layer charging. The near superimposition of the plots demonstrated the reversibility of the Ni^{II}/Ni^{III} couple (Fig. 2). Peak current was proportional to $\upsilon^{-1/2}$ ($r^2 = 0.9998$), and ΔE_p did not change with varying υ. The redox couple was seen to be reversible at scan rates from 20 to 250 mV s^{-1}. Further evidence for the reversibility of this complex lies in the fact that the peak potential difference (ΔE_p) was 110 mV, and the anodic to cathodic peak current ratio ($i_{p,a}/i_{p,c}$) was 1.05 ($\upsilon = 50$ mV s^{-1}). These data suggest that the Ni^{II}/Ni^{III} redox couple behaved as a close to ideal reversible redox couple. Due to this Ni(II) Schiff base's strong redox properties, in conjunction with its methyl sulphide end groups, the complex was further investigated in order to determine whether it could be applied to a gold electrode to act as an electrocatalytically active self-assembled monolayer.

3.2. Characterisation of [Ni(SC$_6$H$_4$NC(H)C$_6$H$_4$ OCH$_2$CH$_2$SMe)(η^5-C$_5$H$_5$)]$_2$ on gold

In order to avoid oxidative S–S coupling in the thiol complex [20], the thiol end groups were protected by a methyl group (Section 2.3). This complex (compound 3, Scheme 1) self-assembled onto gold to yield a monolayer of the thiolato Ni(II) Schiff base. However, before the complex exhibited measurable redox activity, the SAM required voltammetric cycling in 0.1 M NaOH, from -200 to $+600$ mV at 50 mV s^{-1}. Fig. 3 shows the CVs in 0.1 M phosphate buffer solution, pH 7.4, at a SAM-modified gold electrode surface

before and after cycling in alkaline conditions. Prior to cycling in 0.1 M NaOH solution, the SAM showed little or no redox activity with respect to the Ni(II) metal centres. After a single cycle in 0.1 M NaOH, a set of quasi-reversible redox peaks, attributed to Ni oxidation and reduction was observed. When the number of cycles in 0.1 M NaOH was increased, the areas under the anodic and cathodic peaks continued to grow, demonstrating that the number of redox active molecules on the surface of the electrode must have been increasing. Stability was reached after about seven cycles in NaOH, and no further improvement in the peak heights was observed. A reason for this phenomenon can be postulated. It is possible that the desired cleavage of the carbon of the methyl group from the thiol did not occur during the period in which the gold electrode was left standing in deposition solution. Thus, after removal of the electrode from deposition solution, true SAM formation had not occurred, and the complex may have only been bound weakly to the gold, via lone pairs donated by the thiol end groups. This would explain the initially observed poor electronic communication between the Ni(II) redox centres and the gold surface. Subsequent deprotection of the thiol, by electrochemical cycling in 0.1 M NaOH, could result in a change of conformation, with in situ generation of covalent bonding between the sulphur and the gold, for formation of the true SAM. Ultimately, this induced covalent bonding could be the reason for improved electronic communication between the electrode and Ni(II) centres of the complex.

Deprotection of thiol moieties such as CH$_3$ or acyl groups using base has also been used extensively by Tour et al. [20,21]. They have used NH$_4$OH [20] and NaOH [21] to remove the alkyl group so as to minimise oxidative S–S bond formation. These authors found that other bases such as $(n\text{-}C_3H_7)_2$NH or dimethylaminopyridine were less effective in deprotecting the thiol group [20]. Thus, we chose a basic solution of NaOH (0.1 M) for these studies. Deprotection in these previous publications [20,21] was carried out by adding small quantities of base to the SAM deposition solution, so that the complexes became deprotected in the bulk solution, leaving the thiol group free in the presence of the gold substrate for conventional self-assembly. This paper is the first report, to our knowledge, where the protected thiol was allowed to self-assemble onto the gold substrate, *before* using base to promote the S–Au covalent bond. A close-packed SAM will block Faradaic processes from the electrode surface. Cycling the bare gold and the SAM-modified electrode in 0.1 M NaOH solution (Fig. 4) allowed us to evaluate the film ion barrier factor, Γ_{ibf} where

$$\Gamma_{ibf} = 1 - \frac{Q_{SAM}}{Q_{Bare}} \tag{1}$$

where Q_{SAM} and Q_{Bare} are the charges under the gold oxide stripping peaks for the SAM-modified electrode and the bare gold electrode, respectively [22]. An G_{ibf} of unity is an indication that the gold surface is completely isolated from the aqueous solution, which is the oxygen
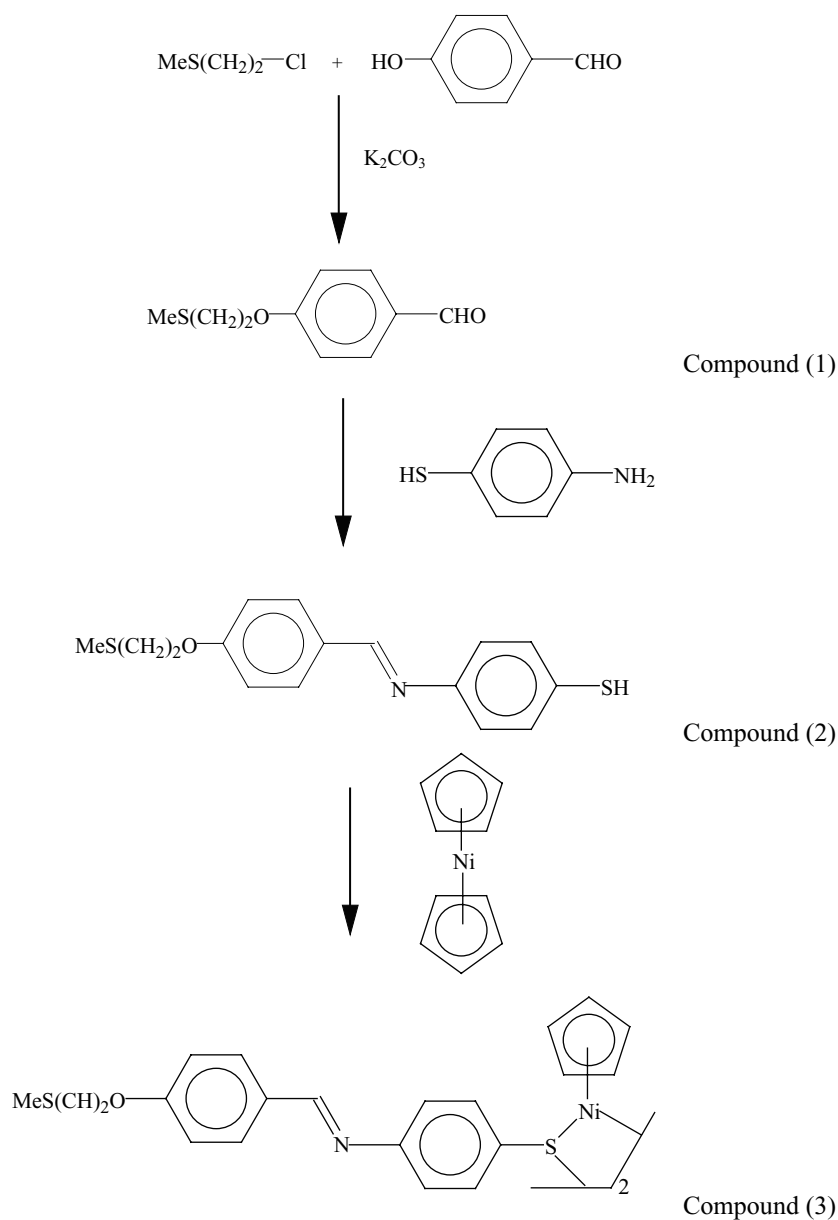
Scheme 1. Reaction scheme for the synthesis of $[Ni(SC_6H_4NC(H)C_6H_4OCH_2CH_2SMe)(\eta^5-C_5H_5)]_2$ complex; where compound 1 is $OHCC_6H_4OCH_2CH_2SMe$, compound 2 is $HSC_6H_4NC(H)C_6H_4OCH_2CH_2SMe$ and compound 3 is $[Ni(SC_6H_4NC(H)C_6H_4OCH_2CH_2SMe)(\eta^5-C_5H_5)]_2$.

source for gold oxide formation. Since no charge could be detected for the gold surface reaction after deposition of $[Ni(SC_6H_4NC(H)C_6H_4OCH_2CH_2SMe)(\eta^5-C_5H_5)]_2$, Γ_{ibf} must be approximately unity indicating that this monolayer provides an excellent barrier to the permeation of electrolyte species [22]. This redox active SAM will block Faradaic processes from the electrode as was shown in Fig. 4, but can also be used for communication between a redox active solution species and the electrode. Fig. 5 demonstrates this principle by showing the CV of the SAM-modified electrode in 1 mM ferrocene, whereby, a mechanism explaining this electrochemical process is given in the inset. ΔE_p for the ferrocene redox couple was calculated to be 79 mV and $i_{p,a}/i_{p,c}$ was 1.This shows that this SAM possesses electro-

catalytic ability to mediate ferrocene, and in theory, any redox couple present in solution. The objective of this work was to develop an efficient electrocatalytic surface for the mediation of enzymatic processes in an electrochemical biosensor, and this result warranted further work.

Verification that it was indeed the SAM layer exhibiting the observed electrochemistry was carried out with a scan rate study. It was observed that anodic current ($i_{p,a}$) was directly proportional to scan rate, ν, consistent with that anticipated for an electrochemical reaction involving a surface confined species ($r^2 = 0.9997$).

For the case of uniformly distributed non-interacting redox centres, located the same distance from the surface of the electrode, for reversible electron transfer reactions, the
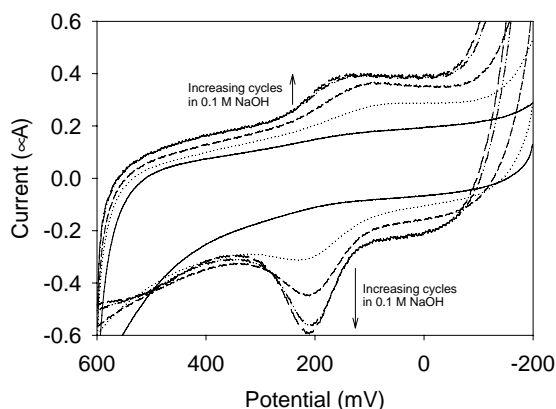
Fig. 3. Cyclic voltammograms of the NaOH-treated SAM-modified Au electrode (1.0 mm diameter) in 0.1 M phosphate buffer, pH 7.4 at a scan rate of 50 mV s^{-1}. Before cycling in NaOH (solid line); after 1 cycle (dotted line), 3 cycles (short dash), 7 cycles (dot and dash) and 15 cycles (long dash) in 0.1 M NaOH.
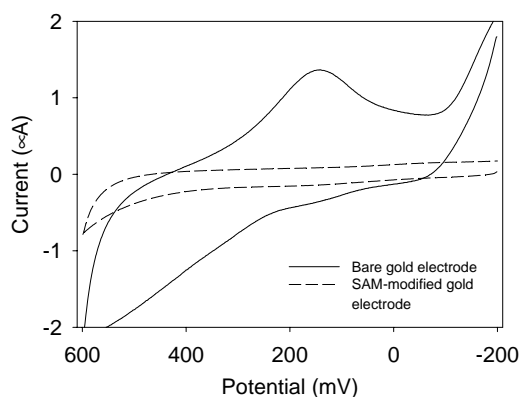

Fig. 4. Cyclic voltammograms in 0.1 M NaOH for bare gold electrode (continuous line) and [Ni(SC$_6$H$_4$NC(H)C$_6$H$_4$OCH$_2$CH$_2$SMe)(η^5-C$_5$H$_5$)]$_2$ SAM-modified gold electrode (dashed line). (WE diameter: 1.0 mm).
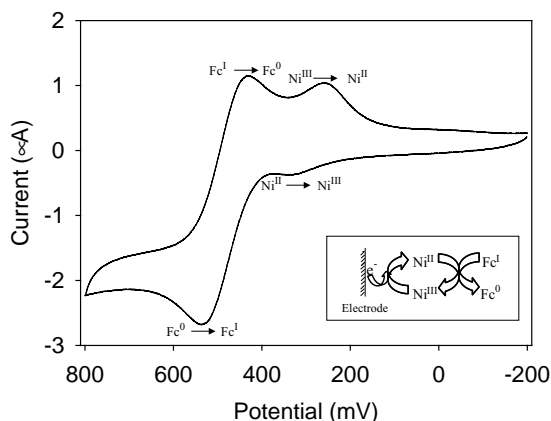

Fig. 5. Cyclic voltammogram of SAM-modified Au electrode in CH$_2$Cl$_2$ containing 1 mM ferrocene and 0.1 M TBATFB (scan rate: 50 mV s^{-1}; WE diameter: 1.0 mm). Inset: schematics for the mediation of ferrocene electrochemistry by the SAM-modified electrode.

anodic and cathodic peaks in a CV, are at exactly the same potential, that is, $\Delta E_p = 0$ mV. Any deviation from this can be assigned to either non-uniformity of the distribution of the redox centres with respect to their distance to the electrode surface, their interactions (e.g. electrostatic repulsions) or to the irreversibility of the charge transfer process involved [23]. Given that in solution, the redox process approaches almost ideal behaviour, (Fig. 2), the quasi-reversible nature (Fig. 3) of the SAM must be attributed to non-uniformity on the surface, or molecular interactions within the SAM.

The $E^{\circ\prime}$ of the SAM-modified electrode was found to vary with pH (evaluated using OSWV in 0.1 M phosphate buffer), with a slope of about -30 mV pH^{-1} over a range of pH 2.5–9.5, which is close to the theoretical value of 29 mV pH^{-1} for a two electron, one proton redox process [24]. This is in agreement with Tafel analysis used to deduce the number of electrons transferred for [Ni(SC$_6$H$_4$NC(H)C$_6$H$_4$OC$_n$H$_{2n+1}$)(η^5-C$_5$H$_5$)]$_2$, where $n = 4$, 14, 16, in bulk solution of CH$_2$Cl$_2$ containing 0.1 M TBATFB. All Tafel plots gave values of approximately two for the number of electrons transferred suggesting the reaction:

$$Ni(A)(II) + e^- \rightarrow Ni(A)(III)$$

$$Ni(B)(II) + e^- \rightarrow Ni(B)(III)$$
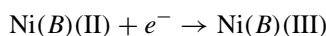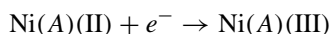
as there are two Ni(II) centres per molecule. The proton redox process that may be occurring was also observed by Ozoemena and Nyokong [22] for an iron phthalocyanine (Pc) immobilised on a gold electrode. This can be attributed to water (in acidic or neutral conditions), and the hydroxyl group (in alkaline conditions) coordinating to the Ni(II) centre. $E^{\circ\prime}$ in 0.1 M phosphate buffer, pH 7.4, was $+202$ mV. This value varied from $+396$ mV in pH 2.5, to a value of $+104$ mV in pH 9.5. Since enzyme will be applied to the surface of the SAM for biosensing, a pH close to neutral was utilised for all further work.

Taking the number of electrons transferred to be two, the surface concentration, Γ, [25] of the nickel redox centres observed from the graphical integration of the anodic wave was found to be 1.548×10^{-11} mol cm^{-2}. This value is quite low, relative to other reported electroactive SAMs [10,22,25], which generally have values one order of magnitude higher than this. Since it has been shown using Eq. (1) that this monolayer is effectively non-permeable to electrolyte species (i.e. surface coverage is probably relatively pin-hole free), the presumption is that not all nickel groups attached to the surface of the electrode are electroactive. One reason for this may be that that not all of the methyl end groups were removed during the voltammetric cycling in NaOH, thus, electronic communication between all of the molecules and the electrode surface could not occur.

3.3. Electrocatalytic reduction of H_2O_2 at the SAM-modified electrode

The objective of this investigation was to develop a suitable SAM-modified electrode for the immobilisation of protein, in order to fabricate an electrocatalytic sensor device. Horseradish peroxidase was used as model enzyme. HRP is a haem-containing glycoprotein that is capable of the catalytic reduction of hydrogen peroxide co-substrate. H_2O_2 induces a catalytic current due to the electrochemical reduction of HRP I and HRP II, which are the two and one oxidation states higher than the native HRP resting state, respectively. HRP was electrostatically attached to the SAM surface by application of an oxidising potential in the presence of HRP ($1\,mg\,ml^{-1}$), to electrostatically adsorb the enzyme to the surface [26,27]. Fig. 6a depicts the CVs of the HRP/SAM-modified electrode in phosphate buffer (pH 7.4), with no H_2O_2 present, in the presence of 50 and 100 mM H_2O_2, under anaerobic conditions. The CVs were performed at the slow scan rate of $5\,mV\,s^{-1}$, to ensure that the fast enzyme kinetics could be monitored. Despite the high background currents in the CVs, electrocatalysis of the Ni(II) was seen. An enhancement of the cathodic Ni(II) peak current was observed in the presence of H_2O_2, consistent with an electrocatalytic effect [13]. This electrocatalytic effect

was not as clear for the anodic peak, however, a small decrease in height was observed, providing extra evidence that the electro-produced Ni(II) was effectively consumed in the enzyme catalysis. There was negligible shift in peak potential on addition of H_2O_2. The same experiment was also monitored using the square wave technique. The voltammograms in Fig. 6b represent the net current (difference between forward and reverse currents) when the electrode was scanned anodically. The high background currents observed in the CVs were eliminated and the decrease in peak current heights upon additions of H_2O_2 was much more pronounced when compared with those observed in CV. This was attributed to the high sensitivity of the square wave technique. Electrocatalysis of the Ni(II) was verified with this result.

In order to confirm the role of the HRP, cyclic voltammograms were carried out on a HRP-free surface. CVs were run before and after addition of H_2O_2. While little or no change in the cathodic peak was observed, an increase in anodic peak current occurred (data not shown). This result indicates that the SAM surface may have the ability to oxidise H_2O_2. However, for the purposes of this report, it can be said that Ni(II) complex alone cannot reduce the H_2O_2, and that HRP is playing an active role. Current responses obtained by the electrocatalytic reduction of H_2O_2 by HRP were monitored using steady state amperometry. Successive additions of H_2O_2 (6.25 mM) to a stirred buffer solution (0.1 M phosphate buffer solution, pH 7.4) were carried out. The effect of applied potential on the catalytic signal and background current of the sensor was tested in the range between +200 and −300 mV versus Ag/AgCl. An optimum ratio of catalytic signal-to-background noise was obtained at a potential of +200 mV. Using an applied potential more positive than +200 mV resulted in oxidation current, due to oxidation of the peroxide by the SAM. Fig. 7 is the peroxide calibration curve for the HRP/SAM-modified electrode where the potential was held at +200 mV. The sensor exhibited typical Michaelis–Menten kinetics. The limit of detection was found to be 6.25 mM, based on a signal to noise
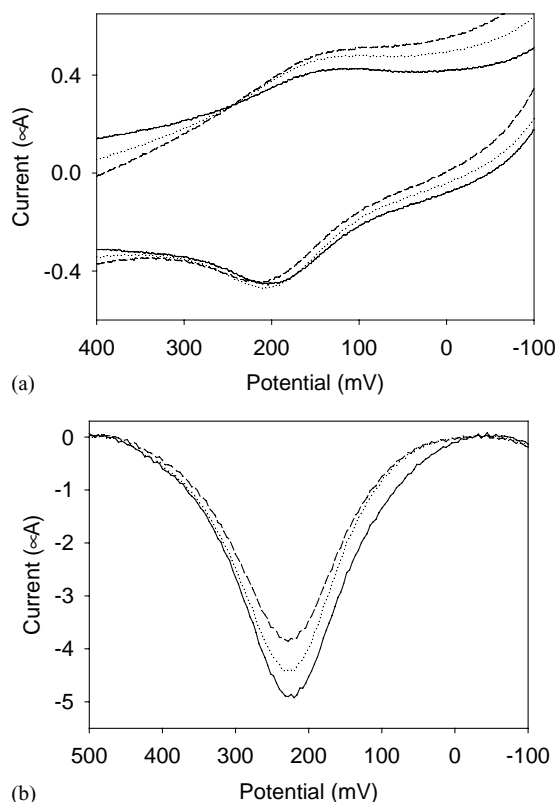

(a)

(b)

Fig. 6. Cyclic (a) and anodic square wave (b) voltammograms of HRP/SAM-modified Au electrode in 0.1 M phosphate buffer, pH 7.4 for 0 mM (continuous line), 50 mM (dotted line) and 100 mM (dashed line) H_2O_2. CV and SWV conditions are as in Fig. 1.
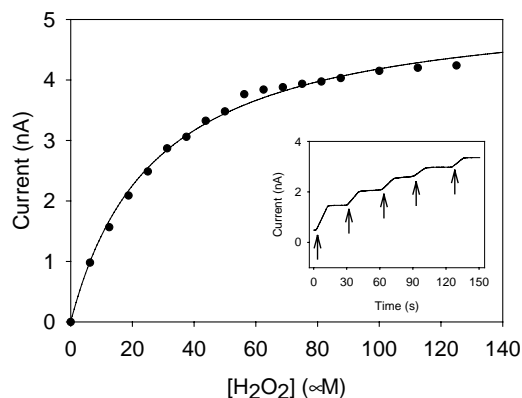

Fig. 7. The H_2O_2 response curve of the HRP/SAM-modified Au electrode at +200 mV vs. Ag/AgCl in 0.1 M phosphate buffer, pH 7.4. Inset: steady state amperogram of the HRP/SAM-modified electrode. Each arrow indicates the addition of 6.25 mM H_2O_2. (WE diameter: 1.0 mm).

(S/N) level of three. The apparent Michaelis–Menten constant, K_m^{app}, was calculated to be 27.25 µM, and the maximum current, I_{max}, was 5.324 nA. Fig. 7 (inset) shows the steady state response observed for the reduction of H_2O_2 at the HRP/SAM-modified electrode in a stirred batch system, in real-time. A stable current response was obtained a few seconds after each H_2O_2 addition. The response time of the sensor was less than 15 s (Fig. 7 (inset)). These are modest characteristics compared to other systems based on electrocatalytic biosensing of H_2O_2. For example, enzyme electrodes based on conducting polymers display particularly high sensitivities with detection limits in the submicromolar range reached. Gaspar et al. [16] recently designed an impressive biosensor based on a novel redox polymer that reached detection limits for H_2O_2 of 25 nM. The authors reported K_m^{app} and I_{max} values of 386 µM and 91 mA, respectively. Other groups have also reported very sensitive peroxidase biosensors based on electrocatalytic surfaces [28,29]. Although our novel approach has not yet reached these detection limits, it does provide advantages over other techniques in that the manner in which the SAM is prepared is an extremely versatile and simple approach for functionalising the electrode surface. This technique can be improved upon by attempts to increase the electroactive nature of the Ni(II) molecules, and by optimising working parameters for enzyme catalysis, such as enzyme loading on the surface of the SAM, pH, adaptation to a flow cell, etc.

4. Conclusions

The fabrication of a SAM of a novel cyclopentadienyl-nickel(II) thiolato Schiff base complex, on a gold electrode is reported for the first time. It was found that the SAM required an activation cycle in 0.1 M NaOH before effective electron communication between the monolayer and the gold surface was obtained. It is likely that an initial scan in alkaline conditions removed the methyl end groups of the Ni(II) complex, thereby, allowing the thiol group to covalently attach to the gold surface in situ to yield a redox active SAM. The monolayer provided effective blocking of Faradaic processes arising from gold surface oxidation. The SAM-modified electrode yielded quasi-reversible electrochemistry with a formal potential of +202 mV in 0.1 M phosphate buffer, pH 7.4. This quasi-reversibility was attributed to non-uniformity of the SAM monolayer, or molecular interactions between the SAM molecules. The surface concentration, Γ, of the nickel redox centres was found to be 9.644×10^{-11} mol cm^{-2}. The formal potential varied with pH to give a slope of about -30 mV pH^{-1}, consistent with a two electron, one proton redox process. Further physical characterisation of this SAM using methods such as electrochemical impedance spectroscopy (EIS) and scanning electron microscopy (SEM) are ongoing, and will be reported at a later date. Electrocatalytic reduction of H_2O_2

at a HRP/SAM-modified electrode was observed. It was observed using CV and OSWV, that the electro-produced Ni(II) complex was effectively consumed in the enzyme catalysis. Steady state amperometry was used to evaluate enzyme kinetics of the biosensor. K_m^{app}, was found to be 27.25 µM and I_{max} was 5.324 nA. The limit of detection was 6.25 µM. Attempts to increase the electroactivity of the SAM by manipulation of the surface using a mixed monolayer approach, or by alteration of the complex itself, will help to improve upon the working parameters of this biosensor. Optimisation of the enzyme parameters will also improve the characteristics of this novel peroxidase-based biosensor. These preliminary results support the view that cyclopentadienyl-nickel(II) thiolate SAMs could prove promising for developing novel electrocatalytic assemblies, especially practical for use in tailoring a variety of amperometric biosensor devices.

References

[1] N. Wilke, A.M. Baruzzi, J. Electroanal. Chem. 537 (2002) 67.
[2] C.R. Raj, K.V. Gobi, T. Ohsaka, Bioelectrochemistry 51 (2000) 181.
[3] N.K. Chaki, K. Vijayamohanan, Biosens. Bioelectron. 17 (2002) 1.
[4] R.G. Nuzzo, D.L. Allara, J. Am. Chem. Soc. 105 (1983) 4481.
[5] R.R. Chellappan, T. Ohsaka, J. Electroanal. Chem. 496 (2001) 44.
[6] K. Kerman, D. Ozkan, P. Kara, B. Meric, J. Gooding, M. Ozsoz, Anal. Chim. Acta 462 (2002) 39.
[7] R. Brito, R. Tremont, O. Feliciano, C. Cabrera, J. Electroanal. Chem. 540 (2003) 53.
[8] C. Danilowicz, J. Manrique, Electrochem. Commun. 1 (1999) 22.
[9] S. Campuzano, R. Galvez, M. Pedrero, F. Manuel de Villena, J.M. Pingarron, J. Electroanal. Chem. 526 (2002) 92.
[10] J. Li, J. Yan, Q. Deng, G. Cheng, S. Dong, Electrochim. Acta 42 (1997) 961.
[11] N. Ho, T. Mak, J. Chem. Soc., Dalton Trans. 12 (1990) 3591.
[12] R.M. Moutloali, PhD Thesis, University of the Western Cape, 2003.
[13] T. Ruzgas, E. Csoregi, J. Emmeus, L. Gorton, G. Marko-Varga, Anal. Chim. Acta 30 (1996) 123.
[14] I. de Mattos, L. Gorton, T. Laurell, A. Malinauskas, A. Karyakin, Talanta 52 (2000) 791.
[15] A. Revzin, K. Shirkar, A. Simonian, M. Pishko, Sens. Actuators, B 81 (2002) 359.
[16] S. Gaspar, I. Popescu, I. Gazaryan, A. Bautista, I. Sakharov, B. Mattiasson, E. Csöregi, Electrochim. Acta 46 (2000) 255.
[17] S. Timur, N. Pazarlloglu, R. Pilloton, A. Telefoncu, Sens. Actuators B 97 (2004) 132.
[18] A. Lindgren, T. Ruzgas, L. Gorton, E. Csöregi, G. Ardila, I. Sakharov, I. Gazaryan, Biosens. Bioelectron. 15 (2000) 491.
[19] T.J. Kemp, Instrumental Methods in Electrochemistry, Ellis Horwood Series in Physical Chemistry, 1990, p. 186.
[20] J. Tour, L. Jones, D. Pearson, J. Lamba, T. Burgin, G. Whitesides, D. Allara, A. Parikh, J. Am. Chem. Soc. 117 (1995) 9529–9534.

[21] J. Tour, A. Rawlett, M. Kazaki, Y. Yao, R. Jagessar, S. Dirk, D. Price, M. Reed, C. Zhou, J. Chen, W. Wang, I. Campbell, J. Eur. Chem. 7 (2001) 5118.

[22] K. Ozoemena, T. Nyokong, Electrochim. Acta 47 (2002) 4035.

[23] P. Krysinski, M. Brzostowska-Smolska, M. Mazur, Mater. Sci. Eng. C 8/9 (1999) 551.

[24] Y. Sato, M. Fujita, F. Mizutani, K. Uosaki, J. Electroanal. Chem. 409 (1996) 53.

[25] D. Li, J. Li, Surf. Sci. 522 (2003) 105.

[26] E.I. Iwuoha, D.S. de Villaverde, N.P. Garcia, M.R. Smyth, J.M. Pingarron, Biosens. Bioelectron. 8 (1997) 749.

[27] A. Morrin, A. Guzman, A.J. Killard, J.M. Pingarron, M.R. Smyth, Biosens. Bioelectron. 18 (2003) 715.

[28] T. Tatsuma, M. Gondaira, T. Wantanabe, Anal. Chem. 64 (1992) 1183.

[29] A. Torriero, E. Salinas, F. Battaglini, J. Raba, Anal. Chim. Acta 498 (2003) 155.